



Supported in part by

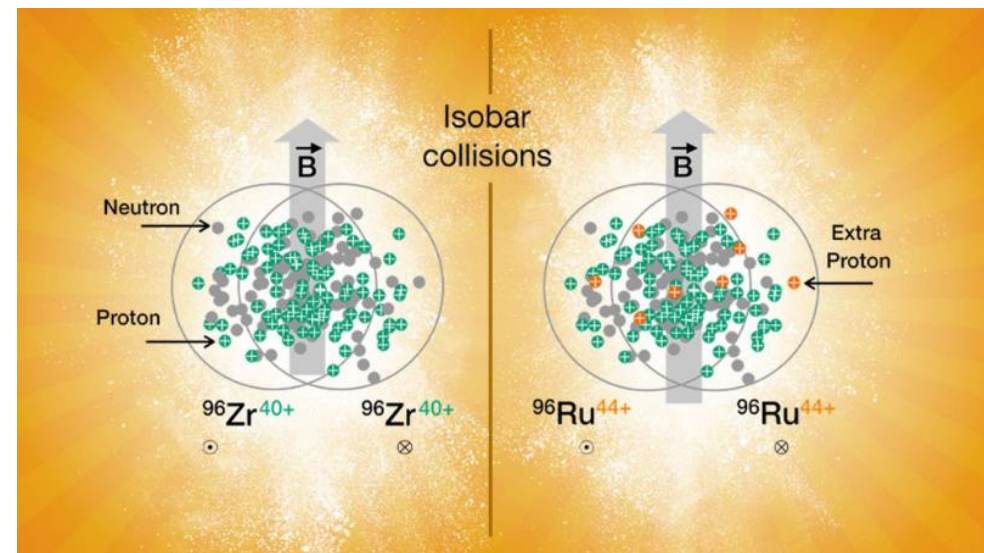
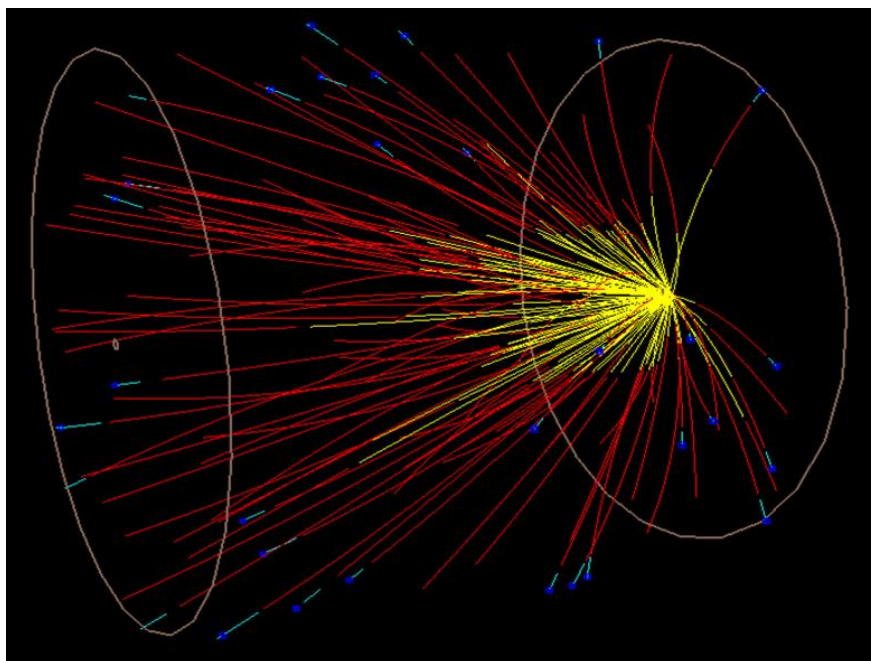
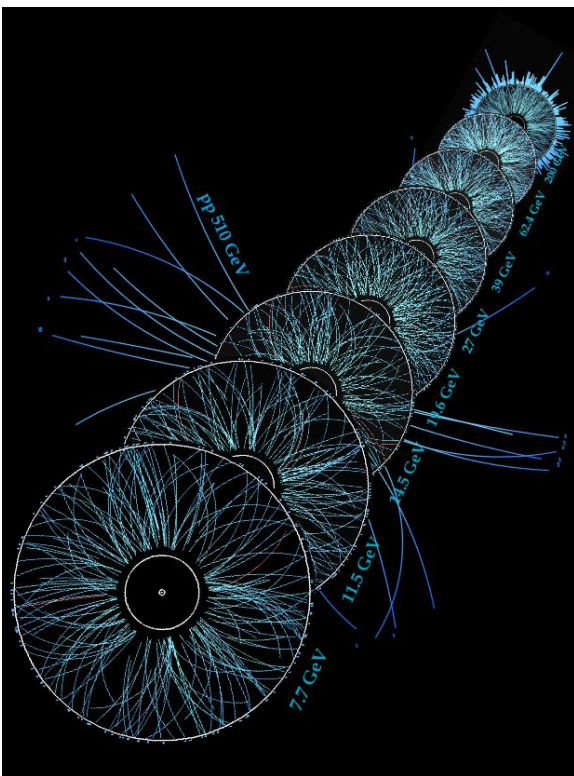
U.S. DEPARTMENT OF
ENERGY



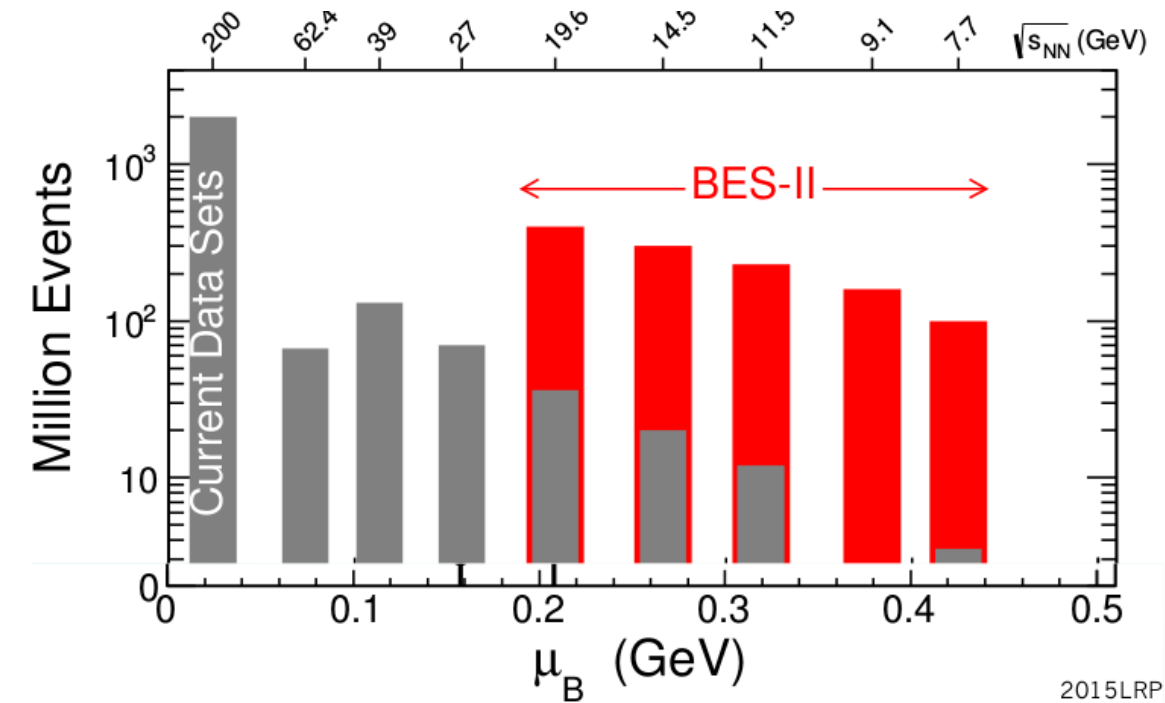
Highlights from the STAR Experiment

Grigory Nigmatkulov

(for the STAR Collaboration)



STAR ☆ BES-I → BES-II



2015LRP

The BES-II program was approved by BNL PAC to take place over the course of two (then three) RHIC running periods

Project listed as a top US NP priority in LRP 2015

BES-I:

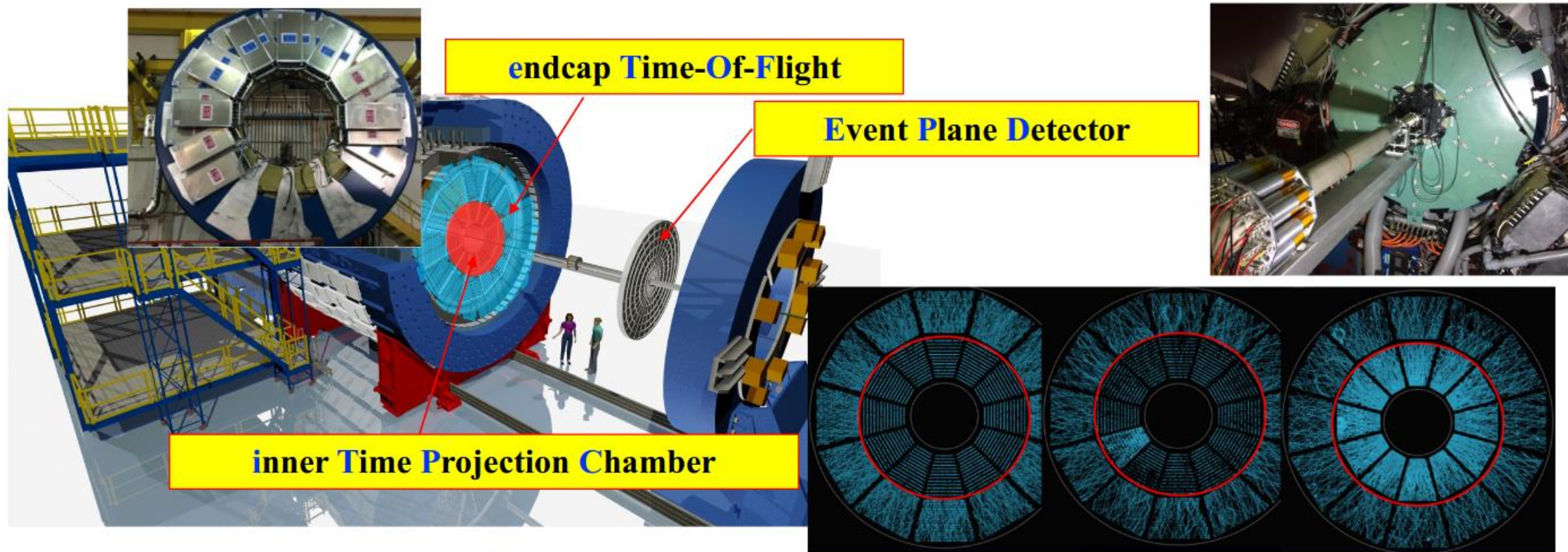
Hints that at low $\sqrt{s_{NN}}$:

- QGP turns off
- Presence of critical point
- Ordered phase transition

BES-II:

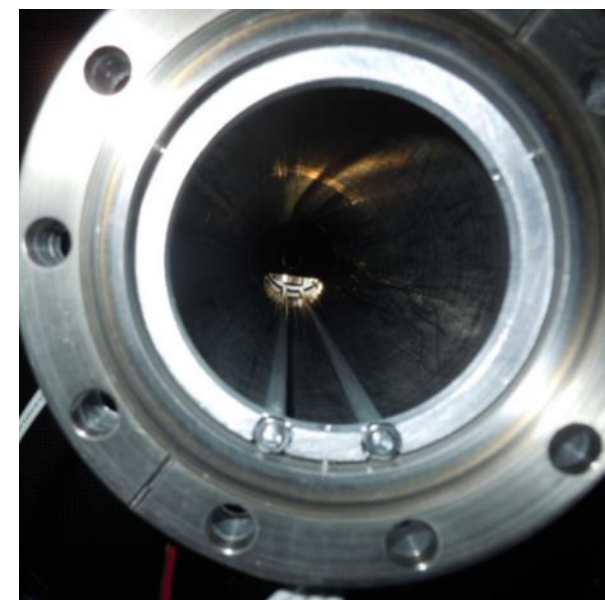
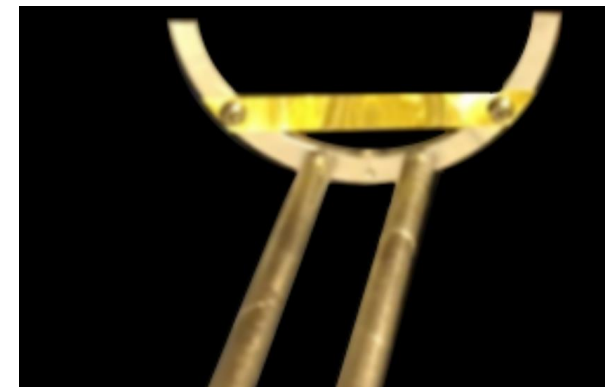
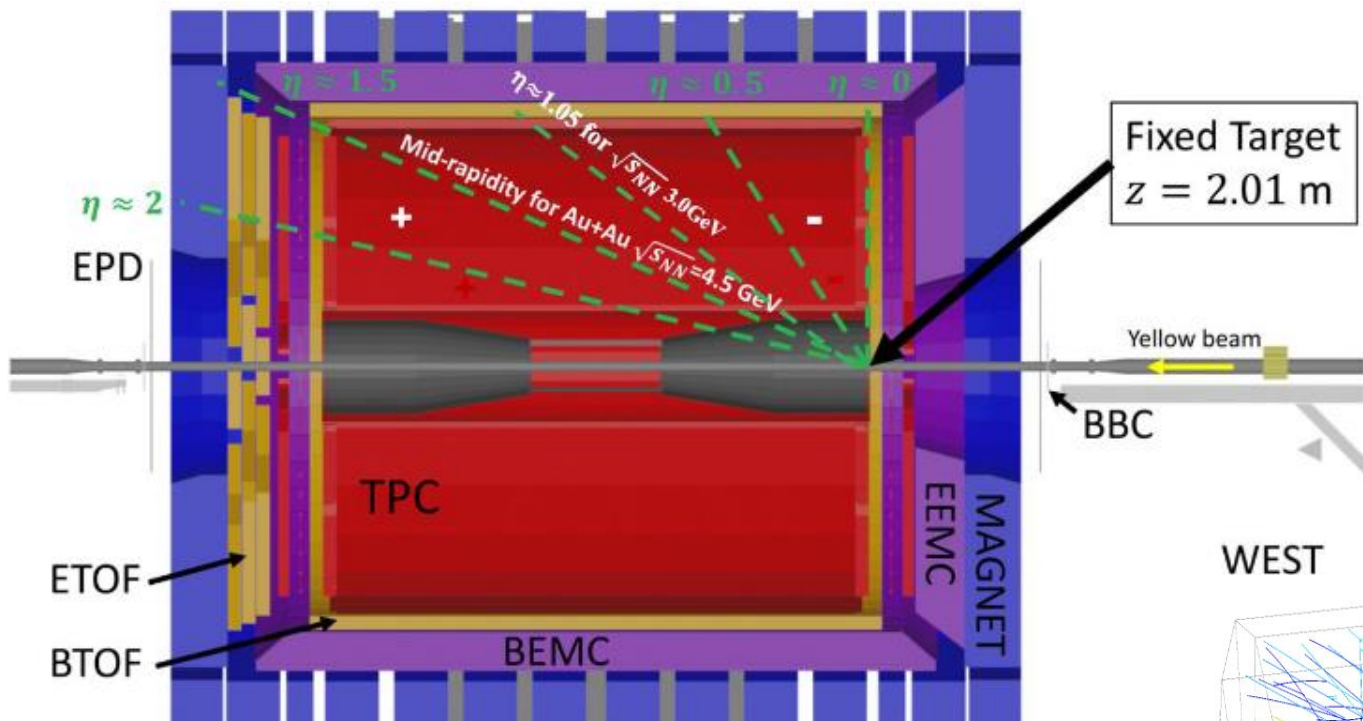
- Need higher statistics
- Need to increase detector acceptance
- Need lower energies
 - Fixed-target (FXT) program
 - Electron cooling of beam

STAR ☆ The BES-II Upgrades



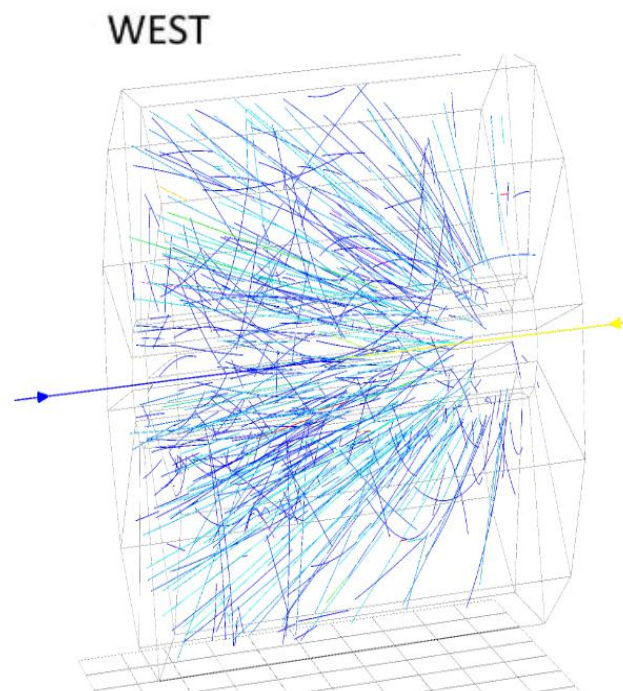
iTPC upgrade	EPD upgrade	eTOF upgrade
$ \eta < 1.5$	$2.1 < \eta < 5.1$	$-1.6 < \eta < -1.1$
$p_T > 60$ MeV/c	Better trigger & b/g reduction	Extend forward PID capability
Better dE/dx resolution Better momentum resolution	Greatly improved Event Plane info (esp. 1 st -order EP)	Allows higher energy range of Fixed Target program
Since 2019	Since 2019	Since 2019

STAR ☆ The Fixed-target (FXT) Setup



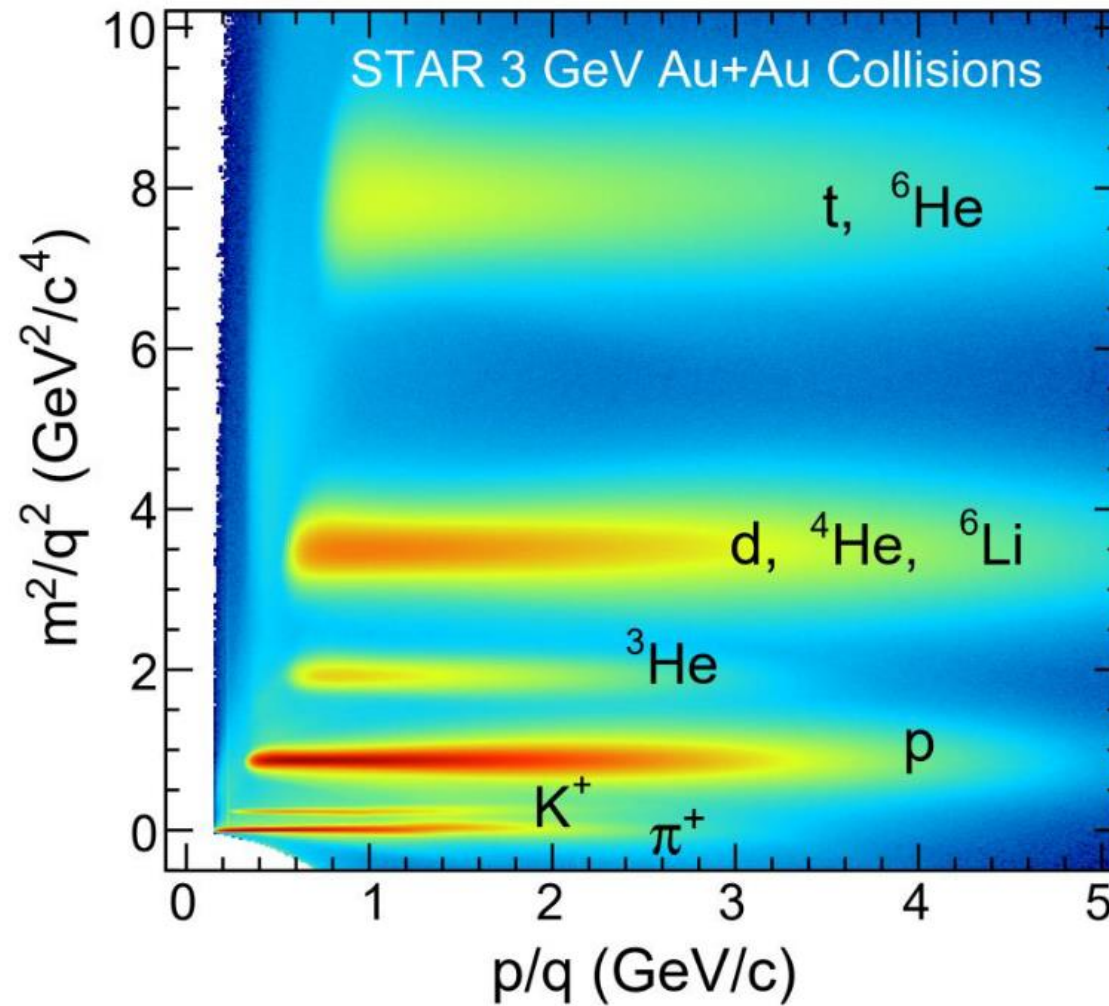
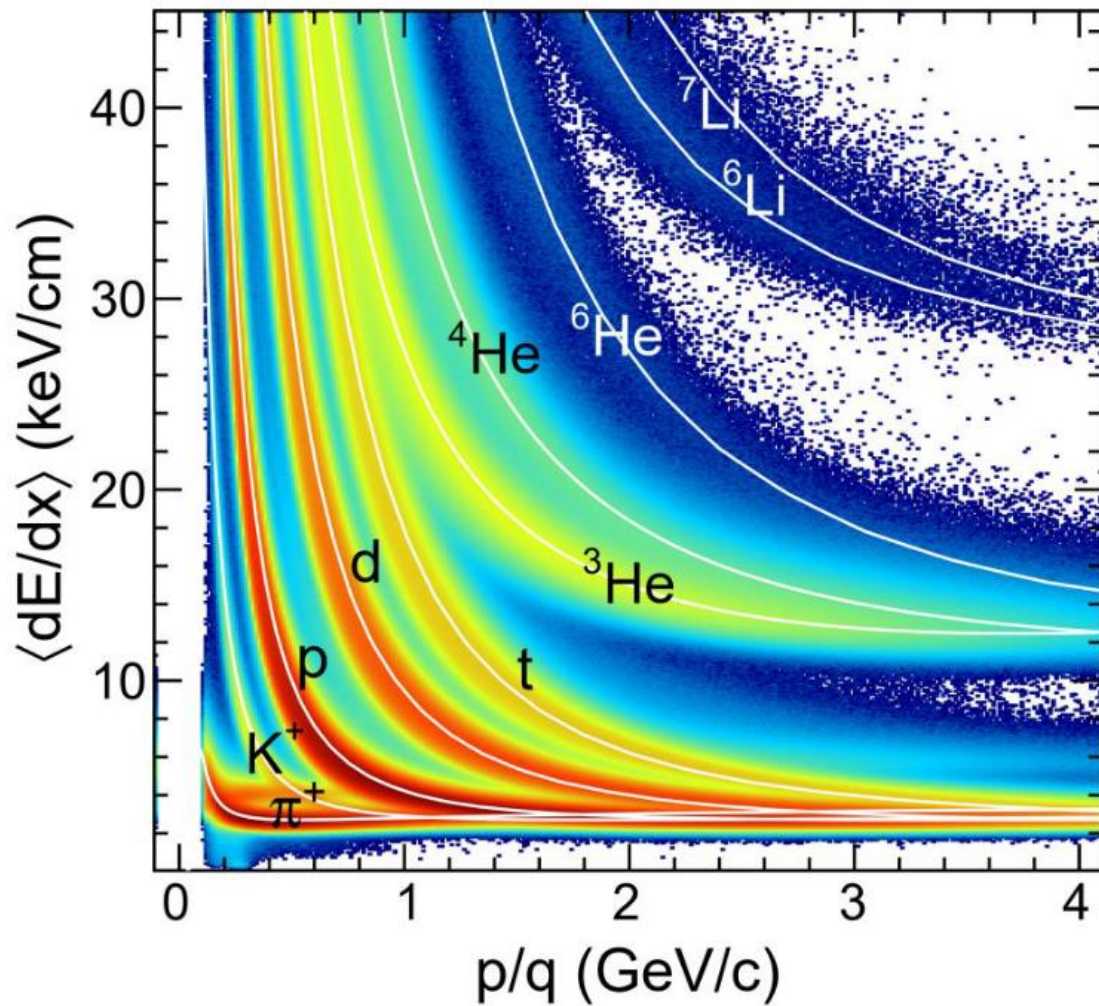
Gold target:

- 2 cm below nominal beam axis
- 2 m from center of STAR
- 250 μm foil





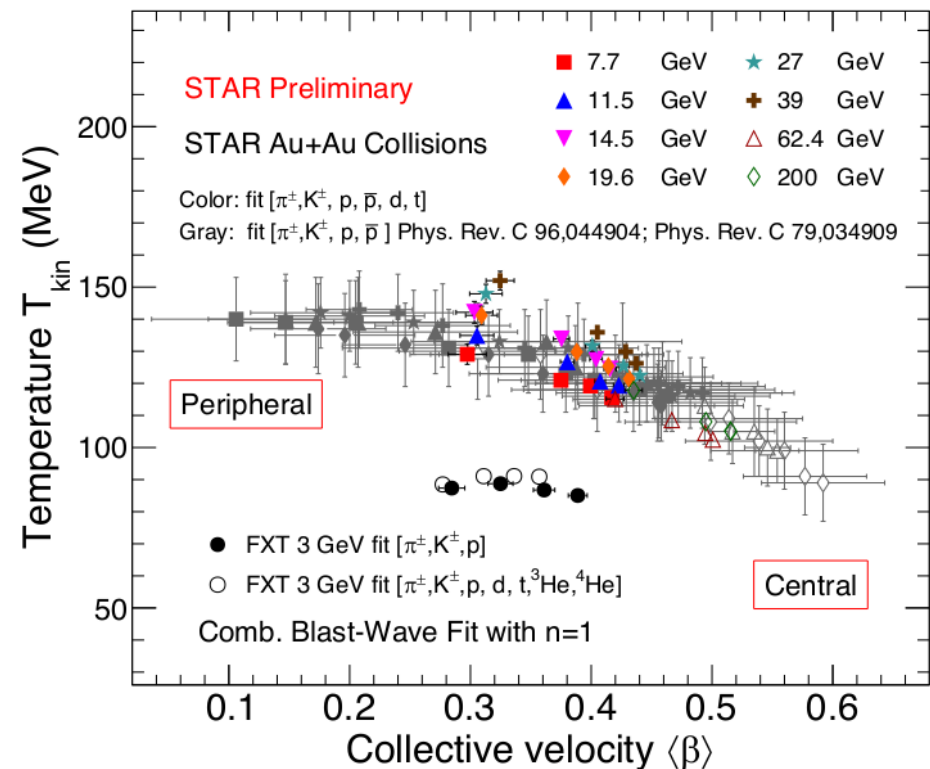
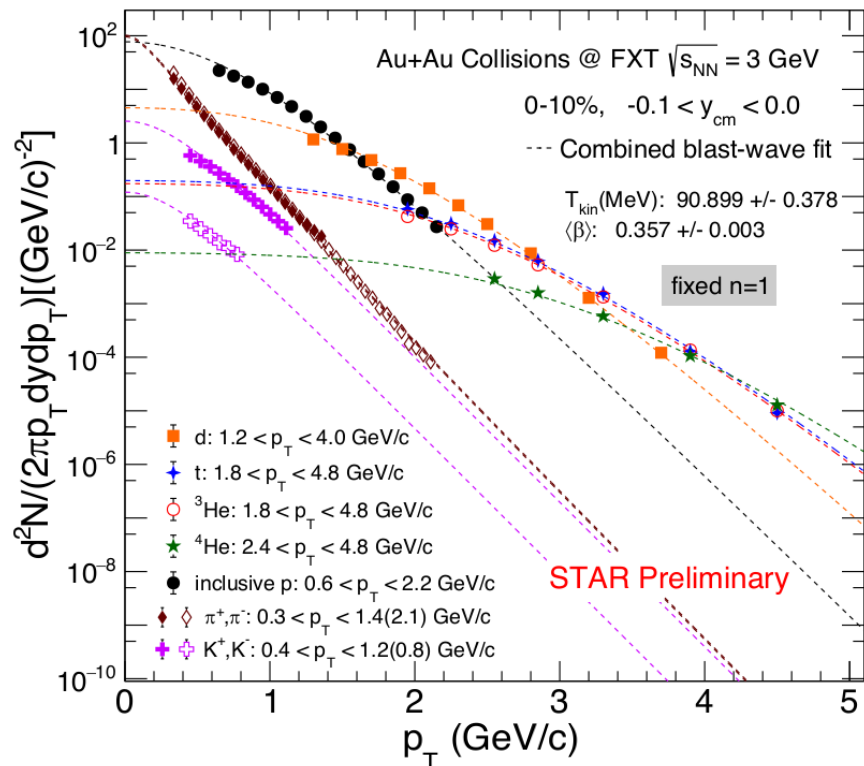
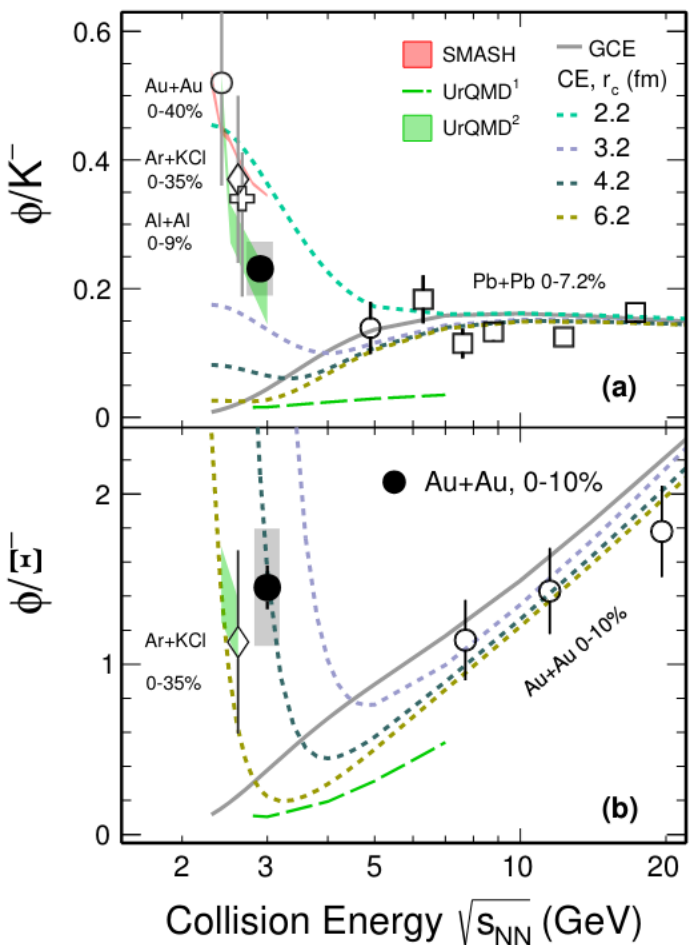
$\sqrt{s_{NN}}$ (GeV)	Beam Energy (GeV/nucleon)	Collider or Fixed Target	$y_{center\ of\ mass}$	μ^B (MeV)	Run Time (days)	No. Events Collected (Request)	Date Collected
200	100	C	0	25	2.0	138 M (140 M)	Run-19
27	13.5	C	0	156	24	555 M (700 M)	Run-18
19.6	9.8	C	0	206	36	582 M (400 M)	Run-19
17.3	8.65	C	0	230	14	256 M (250 M)	Run-21
14.6	7.3	C	0	262	60	324 M (310 M)	Run-19
13.7	100	FXT	2.69	276	0.5	52 M (50 M)	Run-21
11.5	5.75	C	0	316	54	235 M (230 M)	Run-20
11.5	70	FXT	2.51	316	0.5	50 M (50 M)	Run-21
9.2	4.59	C	0	372	102	162 M (160 M)	Run-20+20b
9.2	44.5	FXT	2.28	372	0.5	50 M (50 M)	Run-21
7.7	3.85	C	0	420	90	100 M (100 M)	Run-21
7.7	31.2	FXT	2.10	420	0.5+1.0+ scattered	50 M + 112 M + 100 M (100 M)	Run-19+20+21
7.2	26.5	FXT	2.02	443	²⁺ Parasitic with CEC	155 M + 317 M	Run-18+20
6.2	19.5	FXT	1.87	487	1.4	118 M (100 M)	Run-20
5.2	13.5	FXT	1.68	541	1.0	103 M (100 M)	Run-20
4.5	9.8	FXT	1.52	589	0.9	108 M (100 M)	Run-20
3.9	7.3	FXT	1.37	633	1.1	117 M (100 M)	Run-20
3.5	5.75	FXT	1.25	666	0.9	116 M (100 M)	Run-20
3.2	4.59	FXT	1.13	699	2.0	200 M (200 M)	Run-19
3.0	3.85	FXT	1.05	721	4.6	259 M -> 2B(100 M -> 2B)	Run-18+21



Good particle identification in a broad momentum range using TPC and TOF

STAR Particle Production at 3 GeV

STAR, arXiv:2108.00924



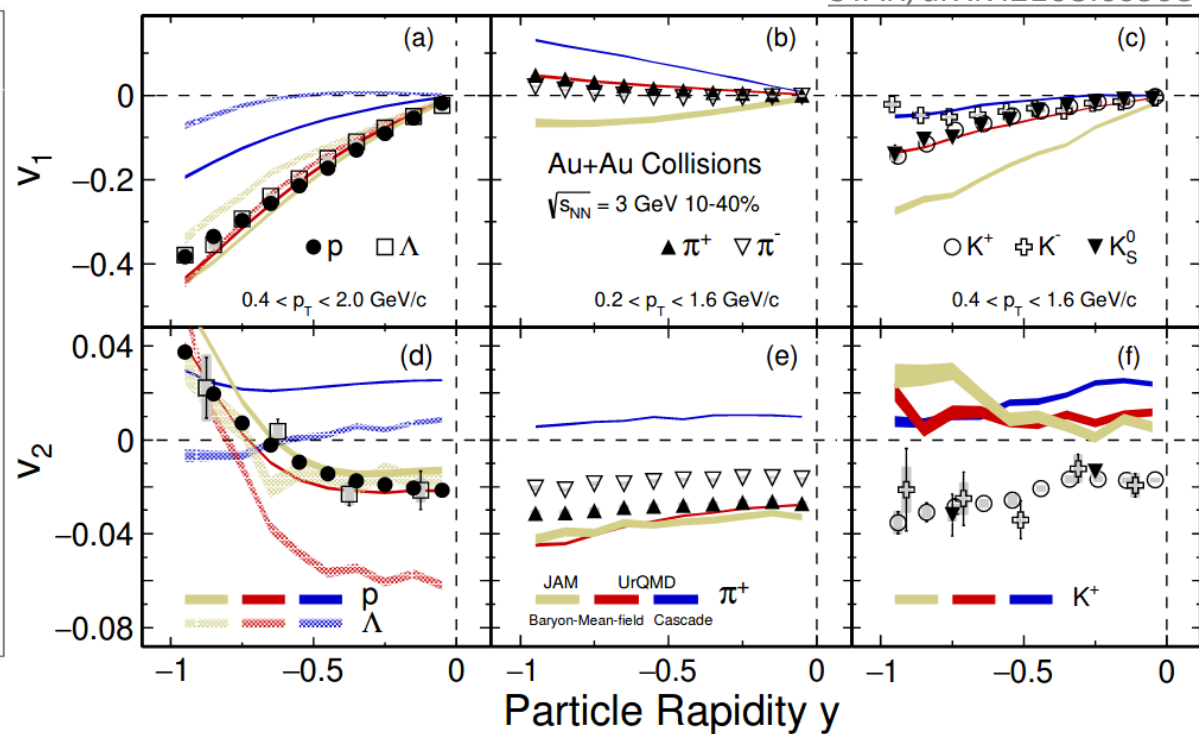
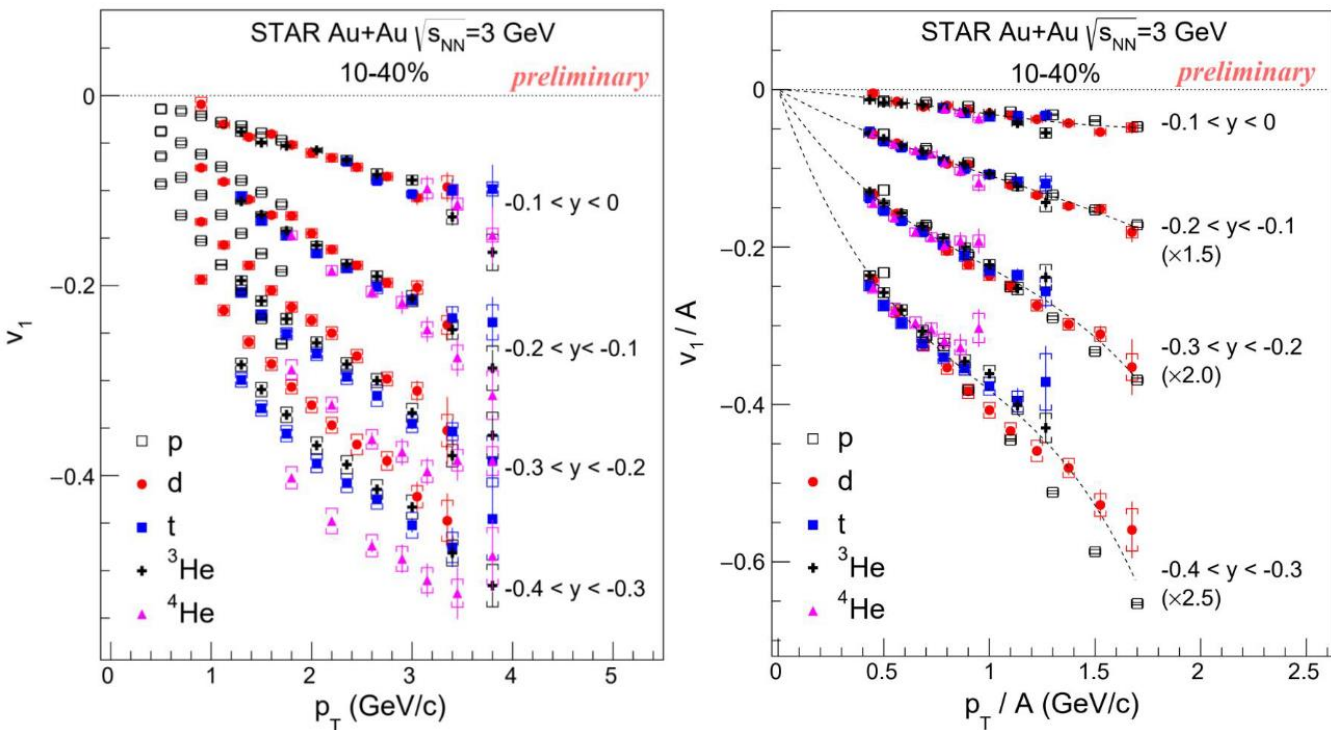
- Light nuclei p_T and rapidity distributions have been extracted
- Midrapidity blast-wave fits:
 - Light nuclei prefer slightly higher T_{kin} , lower β
 - Combined fit to all particles successful

Different trend as compared to higher $\sqrt{s_{NN}}$ - different EOS at 3 GeV?

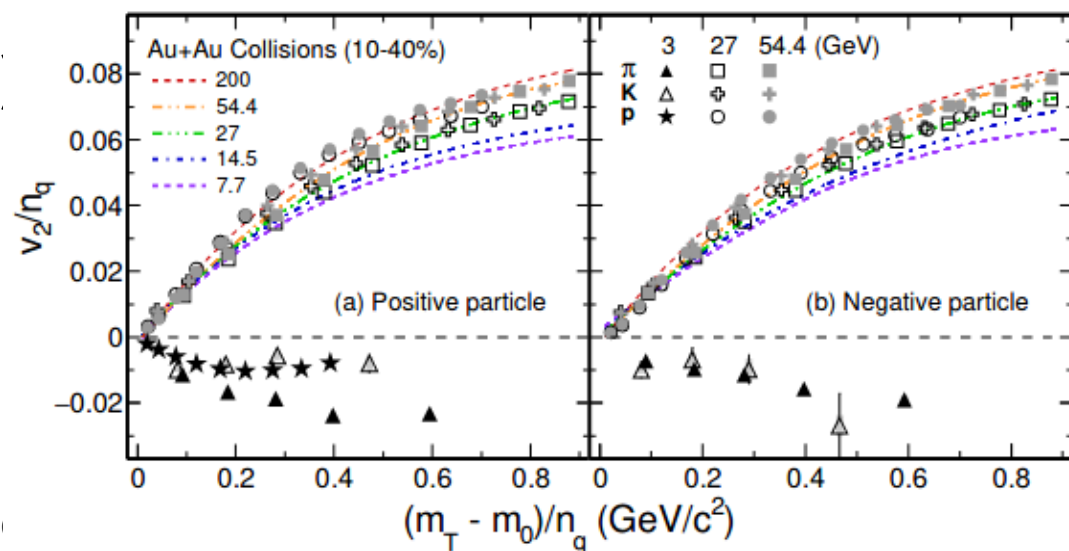
Strange particle ratios indicate the thermal particle phase space at low energies is far from the GCE limit and the local treatment of strangeness conservation is crucial

STAR ☆ Directed and Elliptic Flow

STAR, arXiv:2108.00908



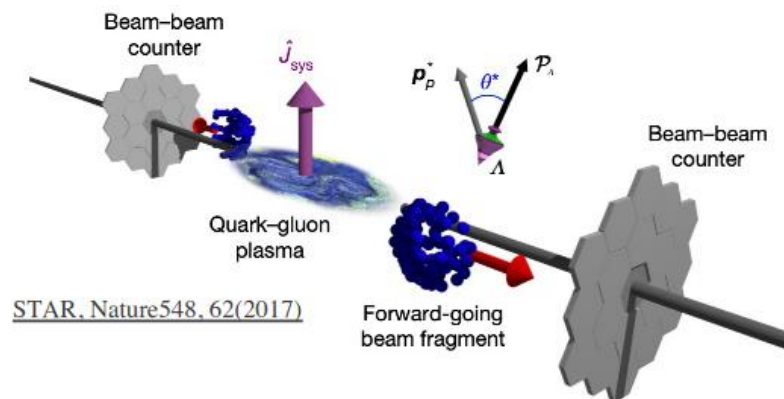
- Light nucleus $v_1(p_T)$ follows atomic-mass-number (A) scaling at different rapidity bins
- Particles and antiparticles are no longer consistent with the single-particle NCQ scaling due to the mixture of the transported and produced quarks



STAR ☆ Global Polarization in BES and FXT

STAR, arXiv:2108.00044

The average vorticity points along the direction of the angular momentum of the \hat{J}_{sys}



Global polarization is measured from the angular distributions of hyperon decay product:

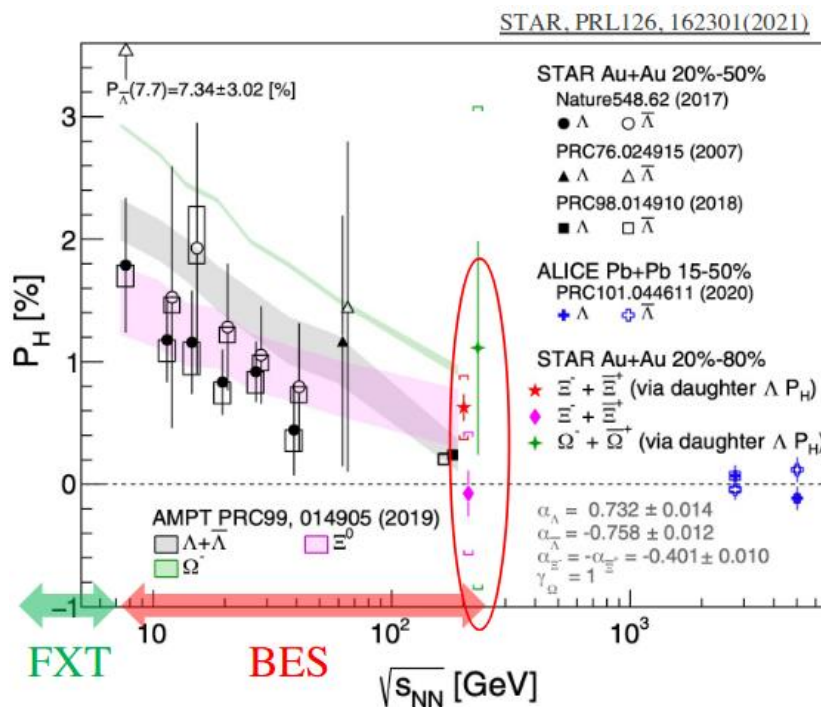
$$P_H = \frac{8}{\pi\alpha_H} \frac{\langle \sin(\Psi_1 - \phi_d^*) \rangle}{\text{Res}(\Psi_1)}$$

Thermal vorticity:

$$\omega = k_B T (P_\Lambda + P_{\bar{\Lambda}}) / \hbar \quad \omega \sim (9 \pm 1) \times 10^{21} \text{ s}^{-1}$$

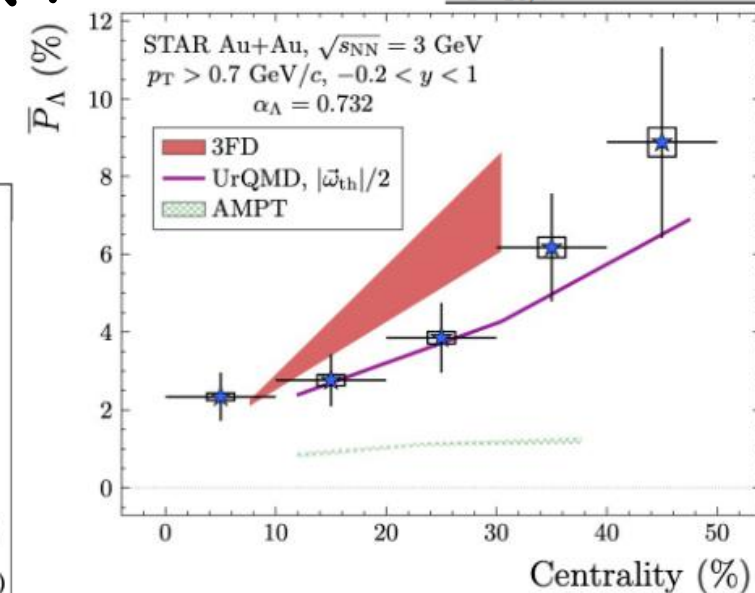
F. Becattini et al., PRC95, 054902(2017)

Opens up new directions in the study of the hottest, least viscous and most vortical fluid matter.



Large angular momentum transferred by the two colliding nuclei

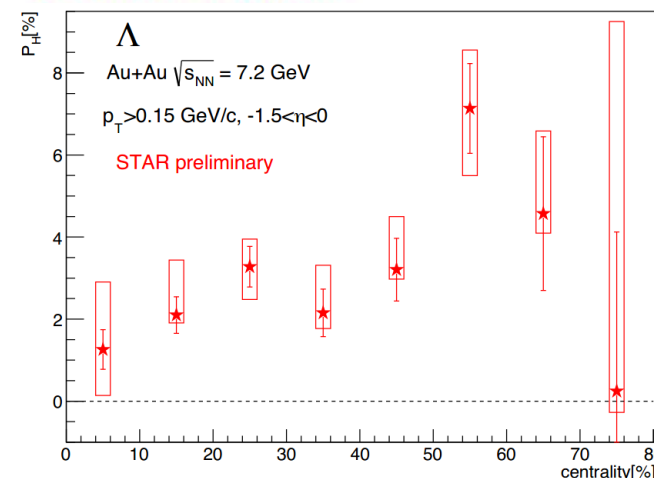
Stronger polarization at lower collision energies.



Much larger \bar{P}_Λ in FXT 3 GeV at 20-50%

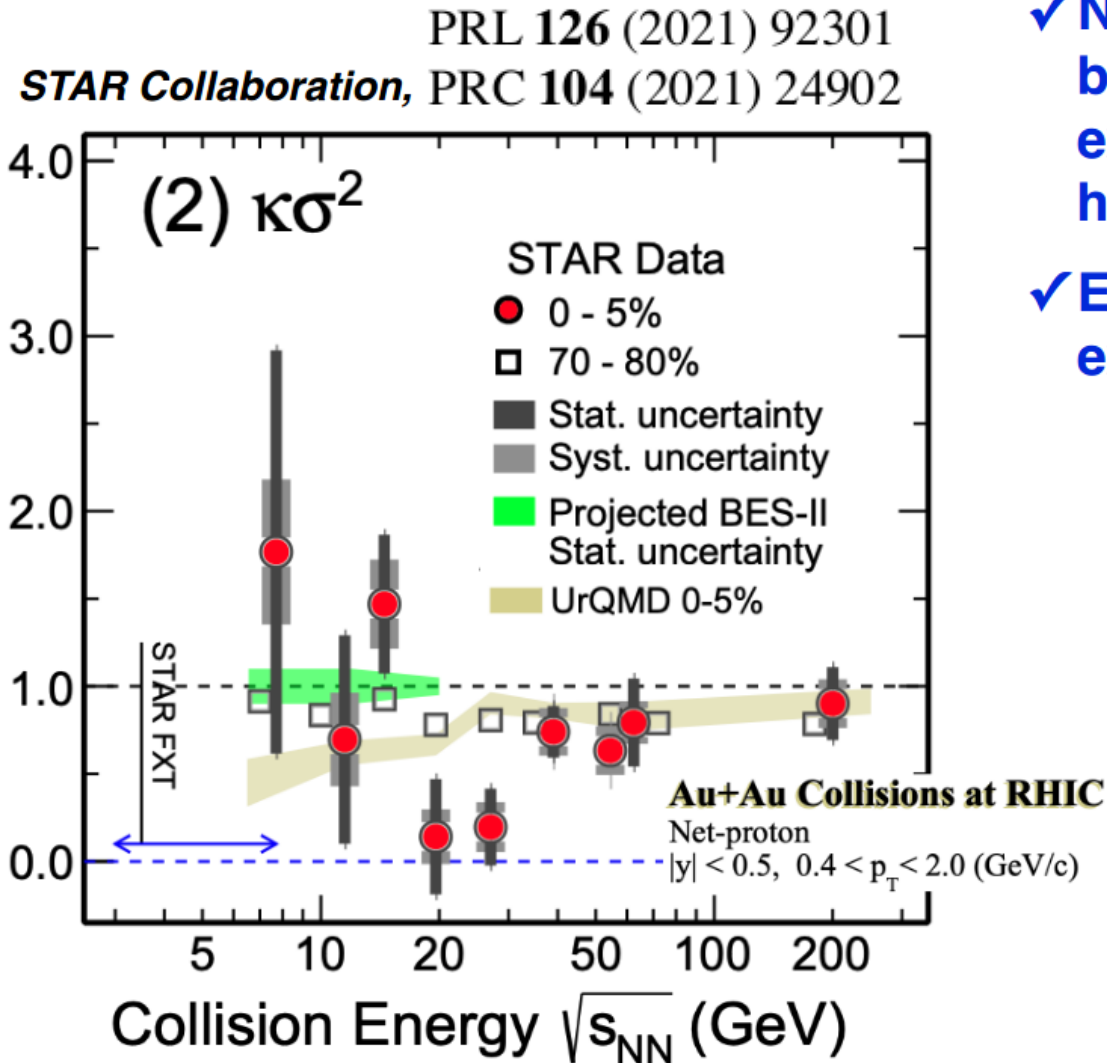
$$4.91 \pm 0.81 \text{ (stat.)} \pm 0.15 \text{ (syst.)} \%$$

Larger hyperon polarization for more peripheral collisions



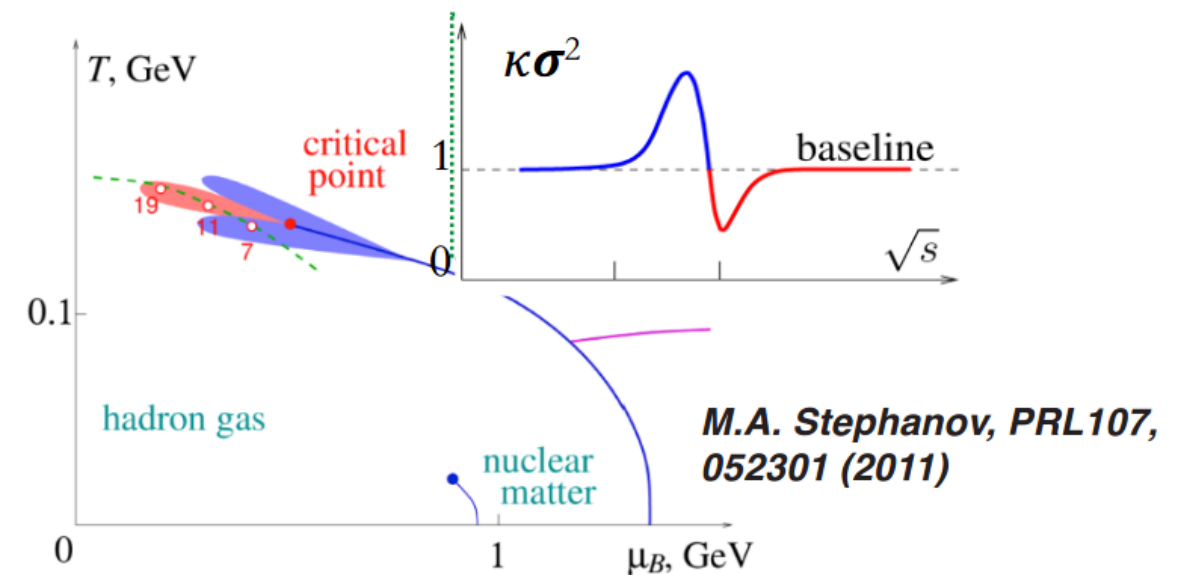
STAR ☆ Hints of Critical Fluctuations

$$\begin{aligned} \langle \delta N \rangle &= N - \langle N \rangle \\ C_1 &= M = \langle N \rangle \\ C_2 &= \sigma^2 = \langle (\delta N)^2 \rangle \\ C_3 &= S\sigma^3 = \langle (\delta N)^3 \rangle \\ C_4 &= \kappa\sigma^4 = \langle (\delta N)^4 \rangle - 3 \langle (\delta N)^2 \rangle^2 \end{aligned}$$



✓ Net-proton $\kappa\sigma^2$ (C_4/C_2) shows a non-monotonic behaviour. The trend is consistent with the expectation from theoretical calculations having a critical point.

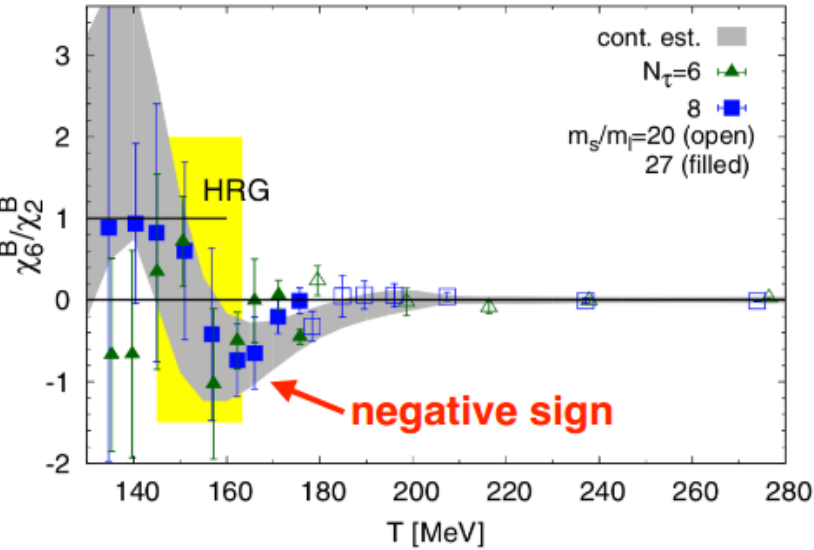
✓ Enhancement at low beam energies cannot be explained by baryon number conservation.



STAR ☆ Hints of Critical Fluctuations

- There isn't yet any direct experimental evidence for the smooth cross over at $\mu_B \sim 0$ MeV
- $C_6/C_2 < 0$ is predicted as a signature of cross over transition
- High-statistics data sets at $\sqrt{s_{NN}} = 27, 54.4, \text{ and } 200$ GeV are analyzed to look for the experimental signature of cross over transition

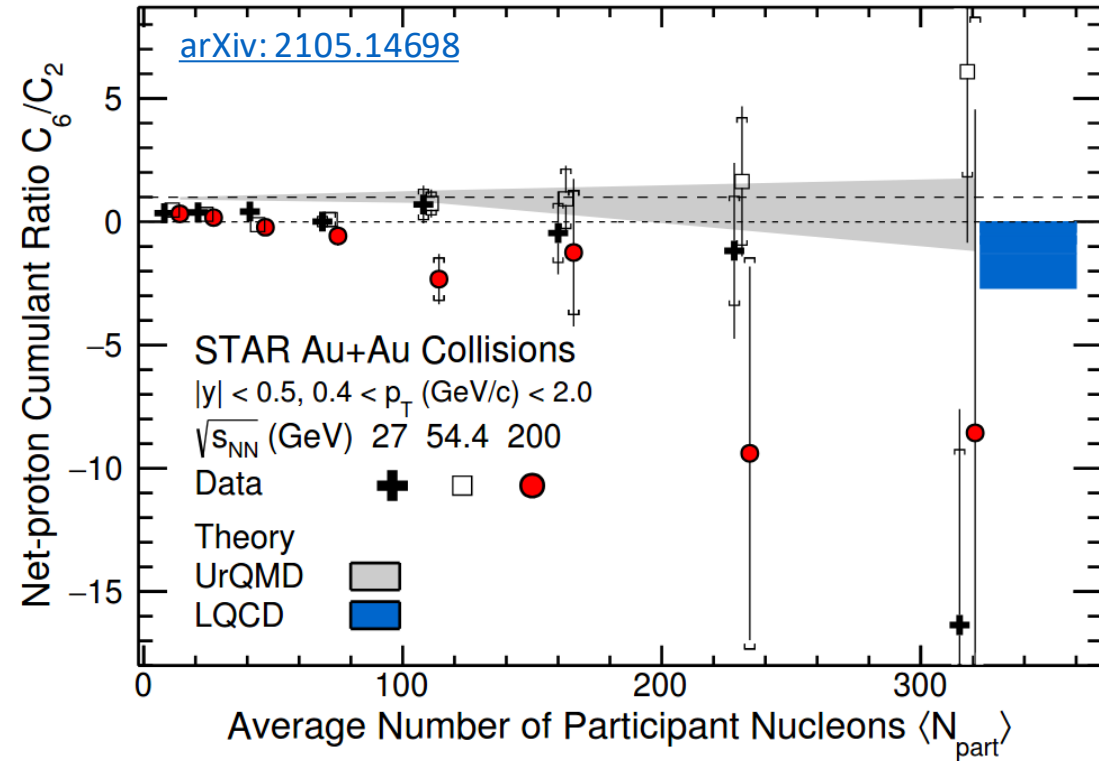
A. Bazavov et al,
PhysRevD.95.054504 : LQCD



C. Schmidt, Prog. Theor. Phys. Suppl. 186, 563–566 (2010)
 Cheng et al, Phys. Rev. D 79, 074505 (2009)
 Friman et al, Eur. Phys. J. C (2011) 71:1694

Freeze-out conditions	χ_4^B/χ_2^B	χ_6^B/χ_2^B	χ_4^Q/χ_2^Q	χ_6^Q/χ_2^Q
HRG	1	1	~ 2	~ 10
QCD: $T^{\text{freeze}}/T_{pc} \lesssim 0.9$	$\gtrsim 1$	$\gtrsim 1$	~ 2	~ 10
QCD: $T^{\text{freeze}}/T_{pc} \simeq 1$	~ 0.5	< 0	~ 1	< 0

Predicted scenario for this measurement



Suggestive of smooth cross over at top RHIC energies

STAR ☆ Hypernuclei Lifetime

- Probe hyperon-nucleon interaction
- Data from $\sqrt{s_{NN}} = 3$ GeV dataset

Λ :

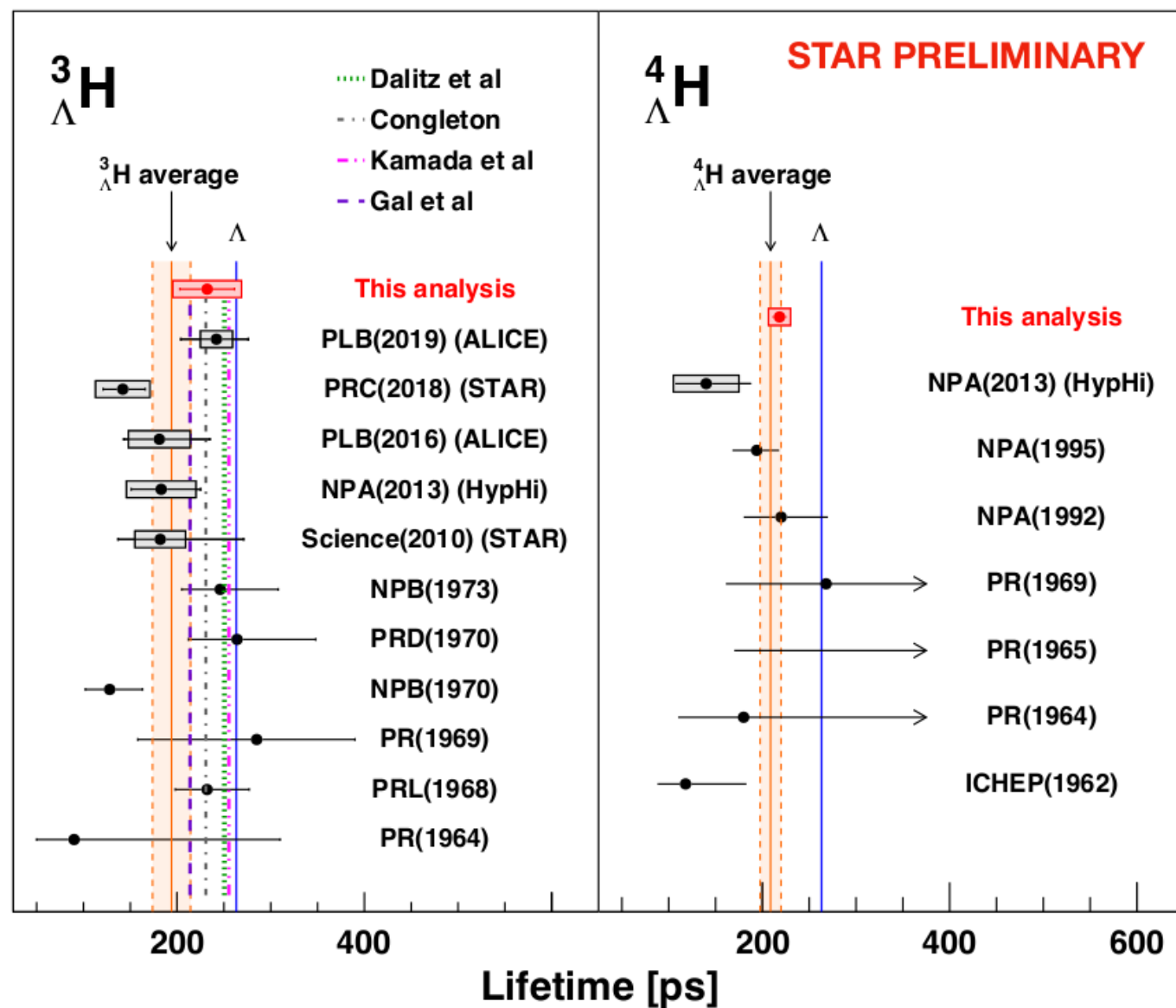
265.0 ± 2.2 ps
(PDG 263.1 ± 2.0 ps)

${}^3_{\Lambda}\text{H}$:

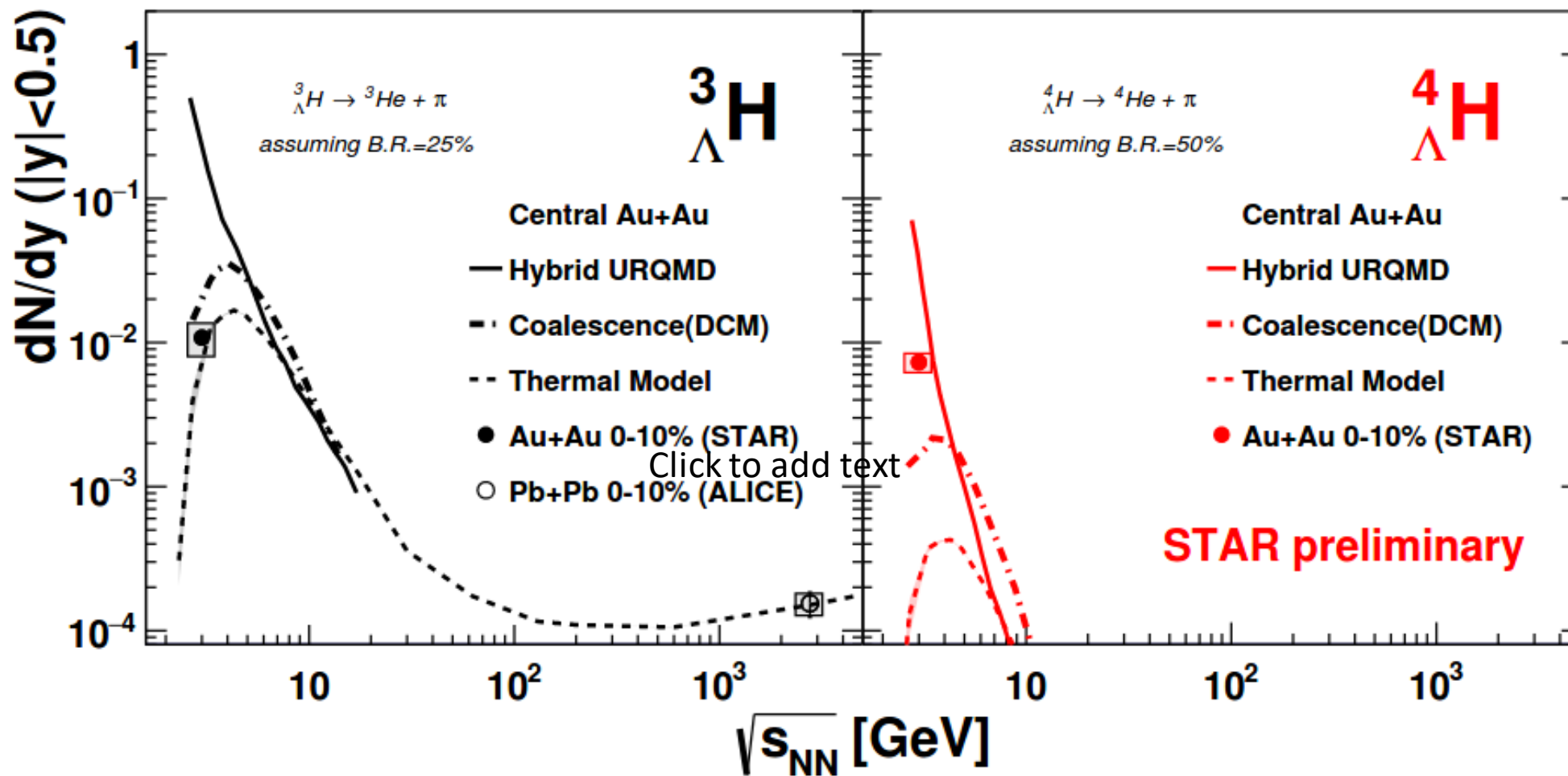
Consistency with
previous results

${}^4_{\Lambda}\text{H}$:

Most precise
measurement to date
Consistency with
previous results

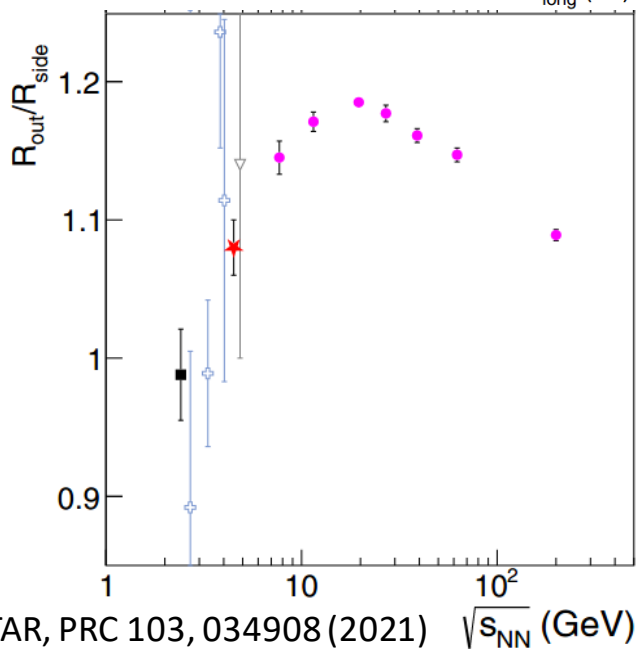
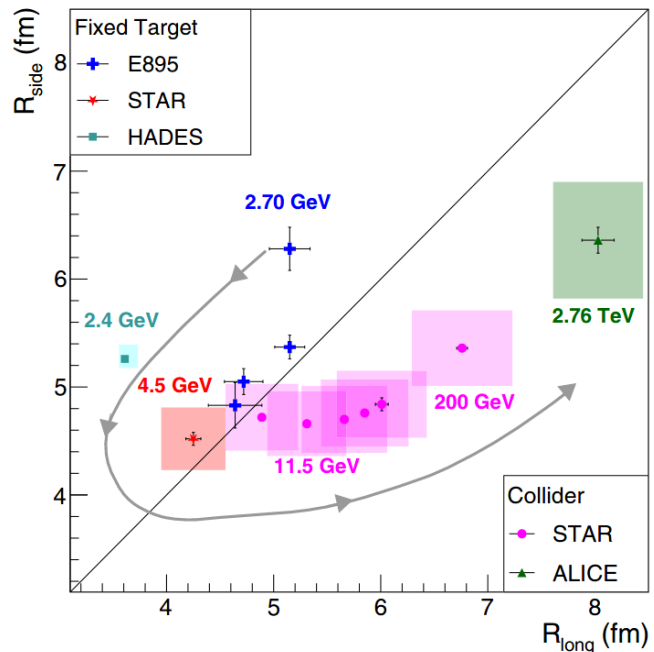


STAR ☆ Hypernuclei Yields

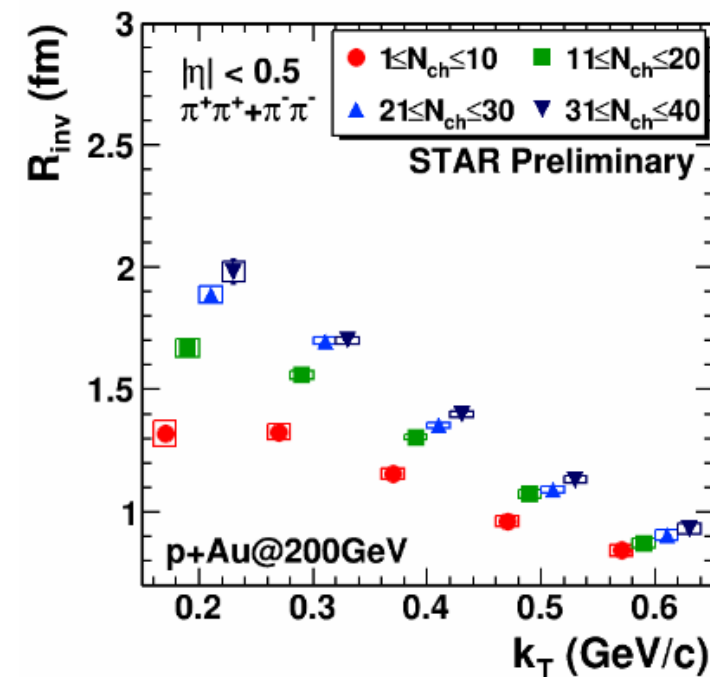
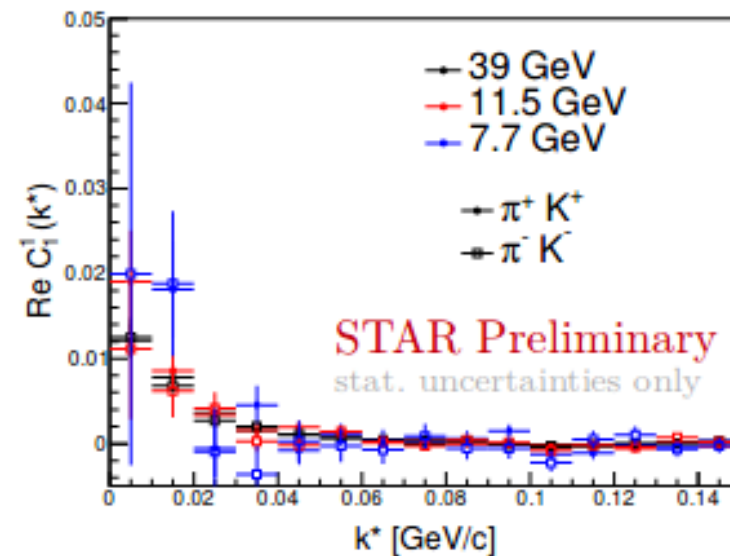


Thermal (with canonical ensemble) and coalescence model calculations
 describe ${}^3_{\Lambda}H$ but not ${}^4_{\Lambda}H$

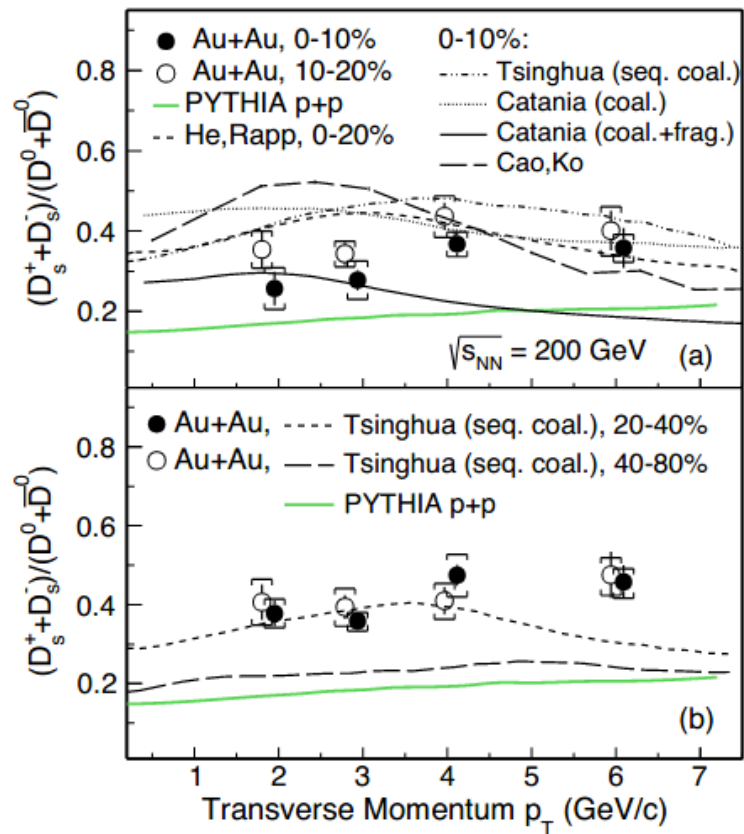
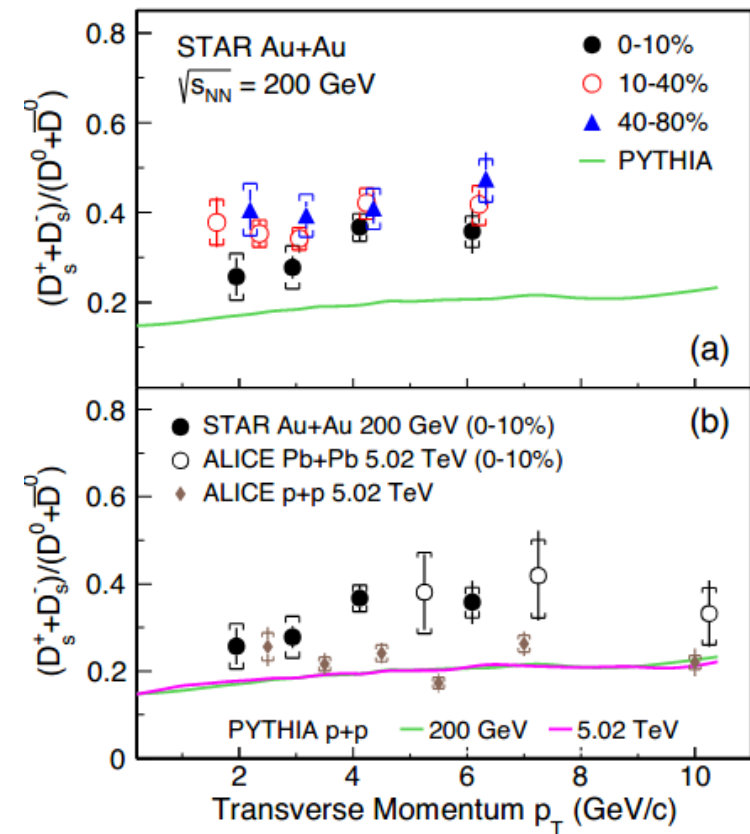
STAR ☆ Femtoscopic Probes



- Sensitivity to the energy dependence of the system dynamics
- Maximum in the $R_{\text{out}}/R_{\text{side}}$ excitation function may occur if system evolves through the 1st-order phase transition
- Collective behaviour in small collision systems



STAR, PRL 127, 092301 (2021)



- Significant enhancement of D_s^\pm/D^0 yield ratio as compared to PYTHIA and p+p at 5.02 TeV
 - No strong centrality dependence
 - Comparable to Pb+Pb at 5.02 TeV
- Models incorporating coalescence with enhanced strangeness production can qualitatively describe data

Catania: Eur. Phys. J. C 78, 348, (2018).

Tsinghua: arXiv1805.10858, (2018).

He, Rapp, Phys. Rev. Lett. 124, 042301 (2020)

Cao, Ko et al.: Phys. Lett. B 807, 135561 (2020).

STAR ☆ Search for the Chiral Magnetic Effect (CME)

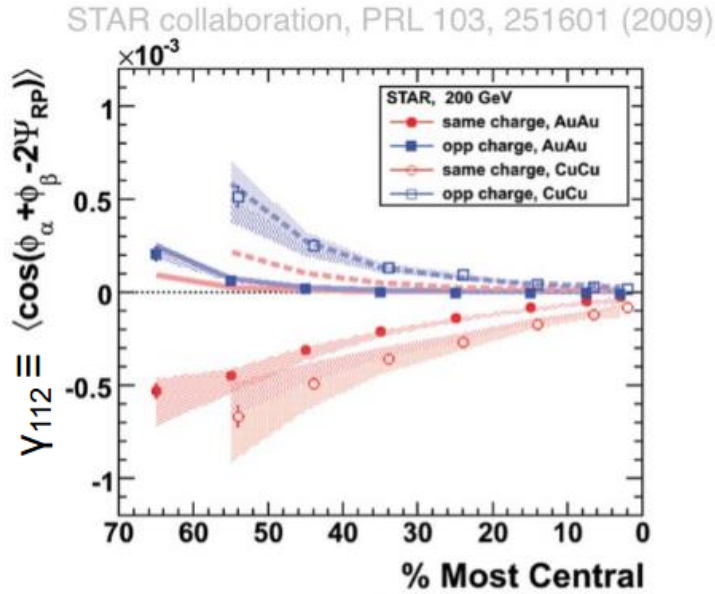
- The chiral magnetic effect (CME) is predicted to occur as a consequence of a local violation of P and CP symmetries of the strong interaction amidst a strong electromagnetic field generated in relativistic heavy-ion collisions.
- Experimental manifestation of the CME involves a separation of positively and negatively charged hadrons along the direction of the magnetic field.
- Previous measurements of the CME-sensitive charge-separation observables remain inconclusive because of large background contributions.
- In order to better control the influence of signal and backgrounds, the STAR Collaboration performed **a blind analysis** of a large data sample **of** approximately 3.8 billion **isobar collisions of $^{96}\text{Ru}+^{96}\text{Ru}$ and $^{96}\text{Zr}+^{96}\text{Zr}$ at $v_{\text{NN}} = 200$ GeV.**

[arXiv:2109.00131](https://arxiv.org/abs/2109.00131)

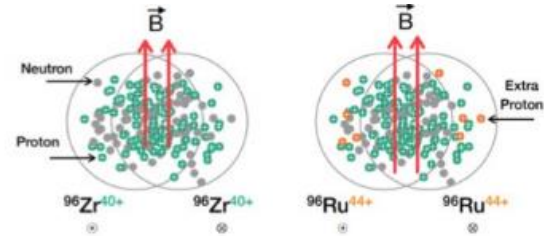
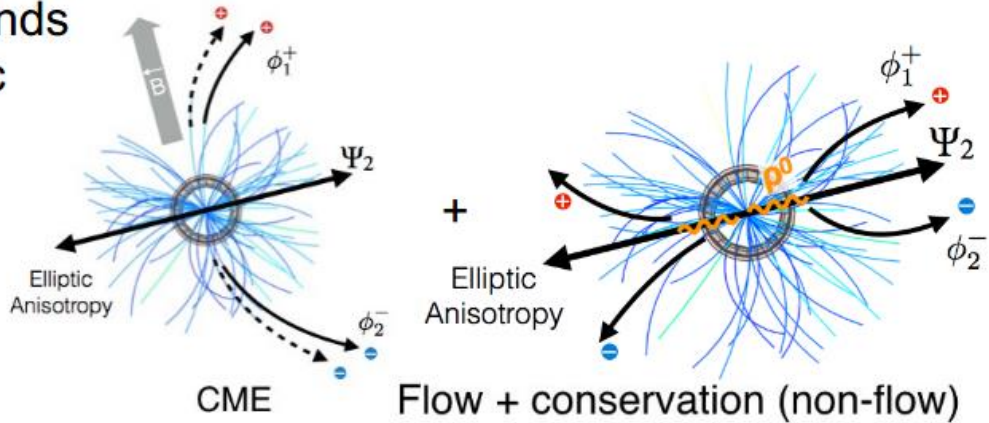
STAR ☆ Search for the CME (History)

First measurements

$$\Delta Y_{112} = Y_{112}^{\text{Opposite Charge}} - Y_{112}^{\text{Same Charge}}$$



Backgrounds can mimic signal

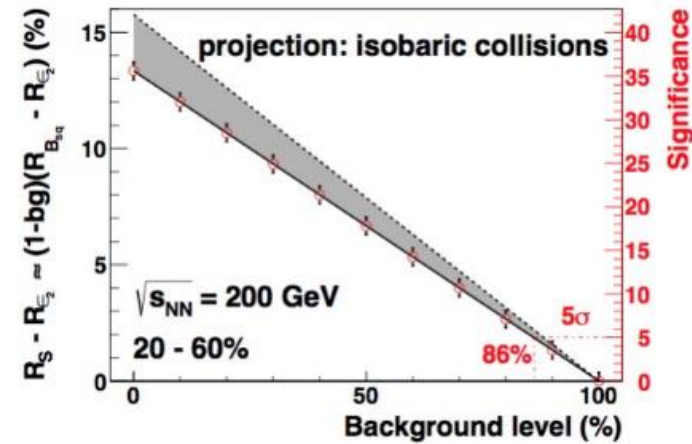


$$\Delta Y^{Ru+Ru} = \Delta Y^{CME} + k \frac{v_2}{N} + \Delta Y^{non-flow}$$

$$\Delta Y^{Zr+Zr} = \Delta Y^{CME} + k \frac{v_2}{N} + \Delta Y^{non-flow}$$

From B-field
10-18% different

Isobar idea:
Change signal while keeping background fixed



2018 Beam Use Request: Would see signal if background contributed up to ~80-85% to measure

Previous measurements of the CME-sensitive charge-separation observables remain inconclusive because of large background contributions.

STAR ☆ Search for the CME (Precision)

Large data set needed to hit small statistical uncertainty target

Systematic uncertainties between species need to be controlled below that level

Special RHIC conditions See G. Marr et al., in 10th International Particle Accelerator Conference (2019) pp. 28–32

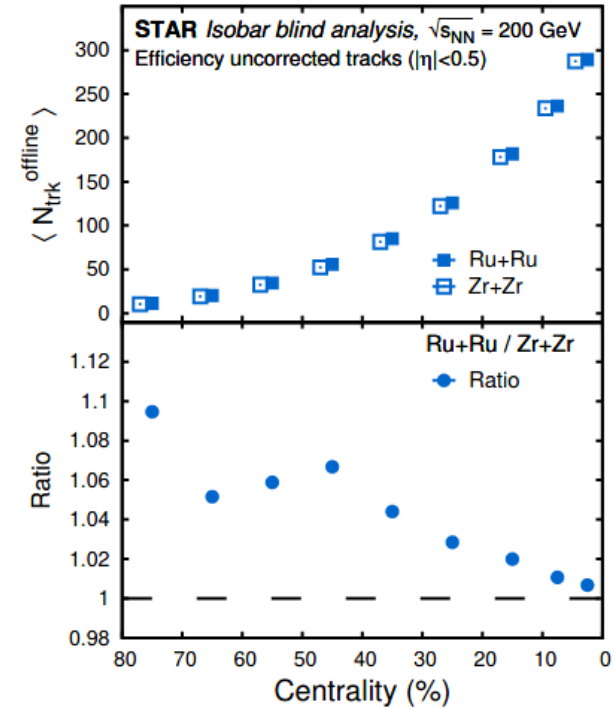
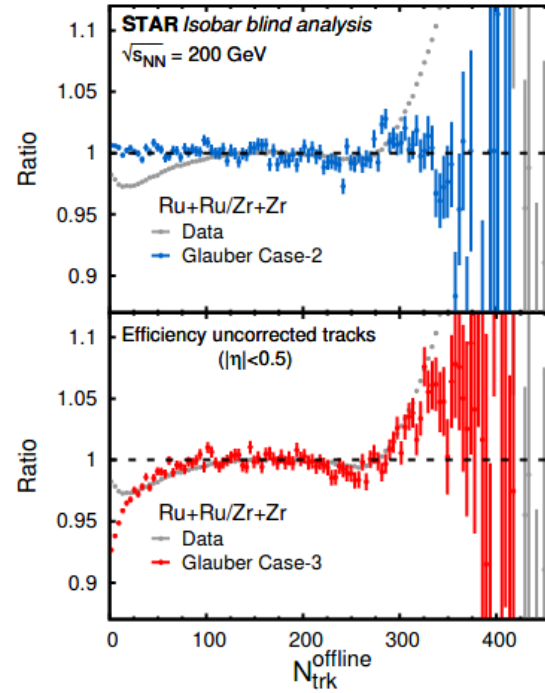
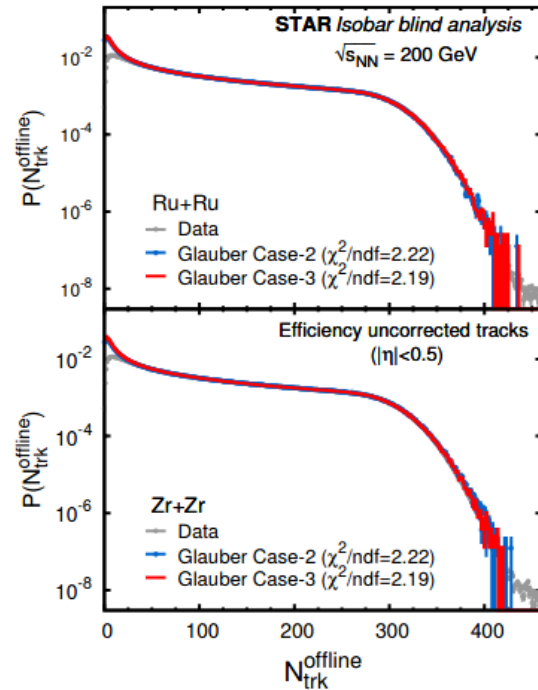
1. Alternate the isobar species between each store of beam in RHIC
2. Keep long stores with constant beam luminosity
3. Match luminosities between the species
4. Adjust the luminosity in such a way that the hadronic interaction rate at STAR is close to 10 kHz.

Precision target achieved:

A precision down to 0.4% is achieved, as anticipated, in the relative magnitudes of the pertinent observables between the two isobar systems

STAR Search for the CME (Centrality)

[arXiv:2109.00131](https://arxiv.org/abs/2109.00131)

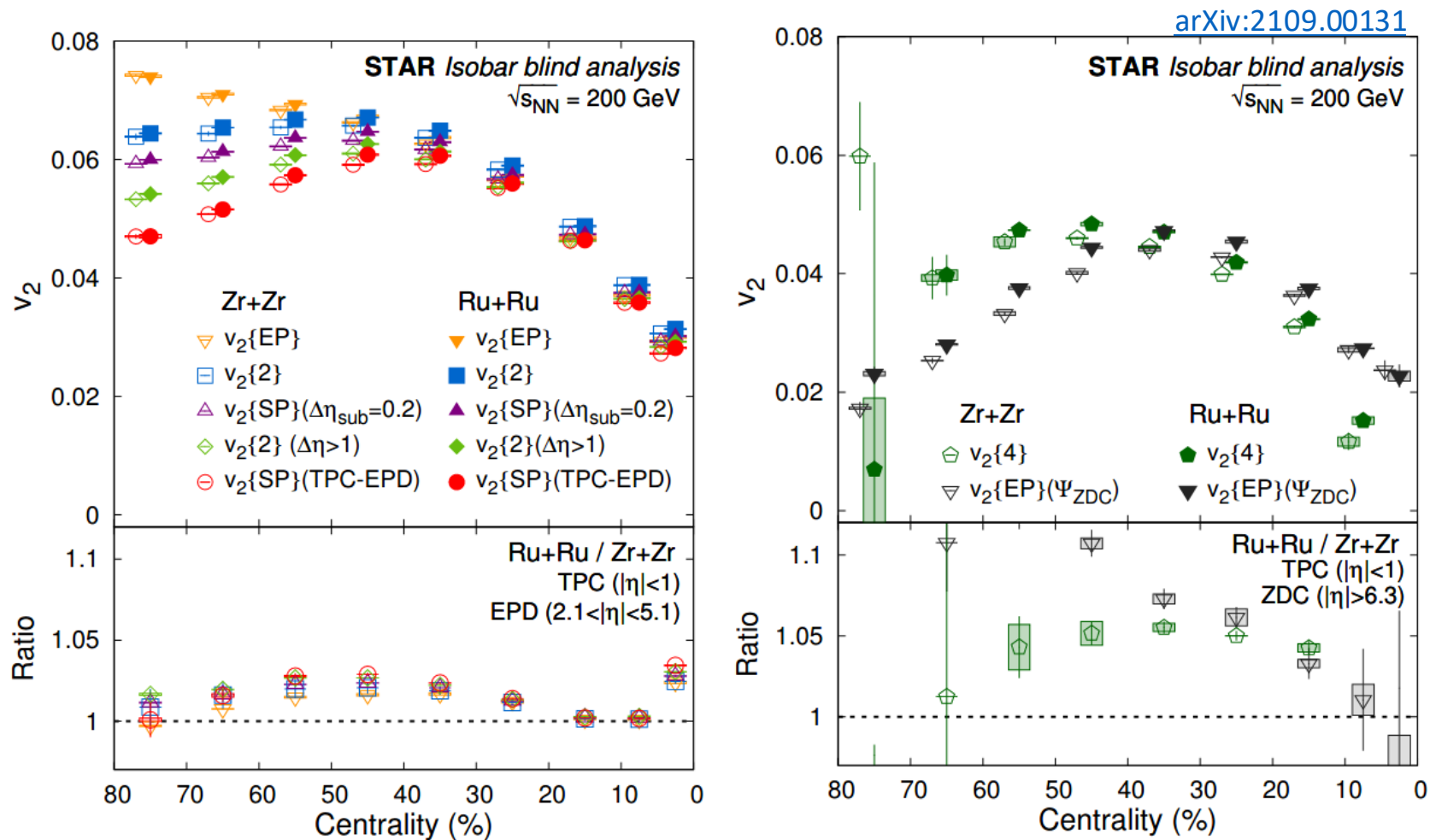


- The 3 sets of Woods-Saxon parameters from the literature have been studied
 - Fit to the multiplicity distributions using the two-component nucleon-based Monte Carlo Glauber
 - Best fit from Case-3: different neutron skin without quadrupole moments

Nucleus	Case-1 [83]			Case-2 [83]			Case-3 [113]		
	R (fm)	a (fm)	β_2	R (fm)	a (fm)	β_2	R (fm)	a (fm)	β_2
$^{96}_{44}\text{Ru}$	5.085	0.46	0.158	5.085	0.46	0.053	5.067	0.500	0
$^{96}_{40}\text{Zr}$	5.02	0.46	0.08	5.02	0.46	0.217	4.965	0.556	0

- Result: difference in multiplicity at matching centrality

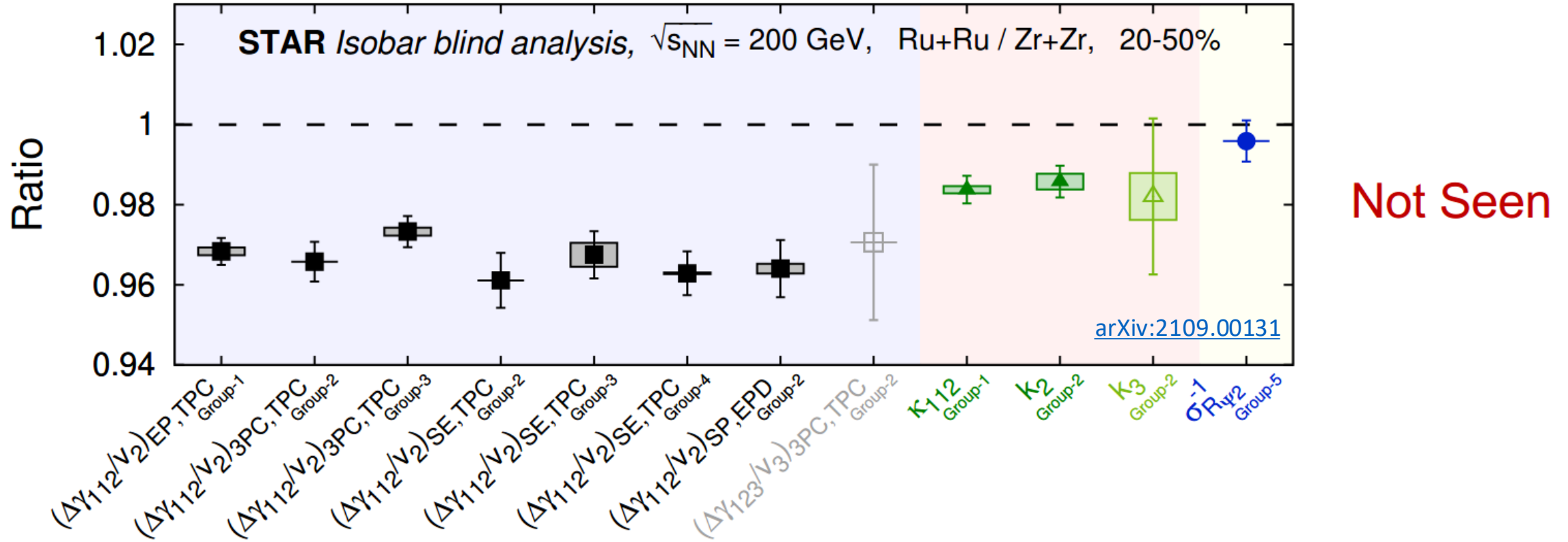
STAR Search for the CME (Crosschecks)



Observed differences in the multiplicity and flow harmonics at the matching centrality suggest that the magnitude of the CME background is different between the two species

STAR ☆ Search for the CME (Results)

Predefined CME signatures: ratios involving $\Psi_2 >$ those involving Ψ_3 , and > 1



No CME signature that satisfies the predefined criteria observed

Note: other measurements in paper that I don't have time to show in this talk

(spectator-participant analysis for CME signal fraction, $\Delta\eta$ dependence of correlations, ...):

All come to this conclusion

STAR ☆ Summary

Presence:

- BES-II upgrades performing at or above expectation
- Excellent performance from RHIC and STAR
- All requested BES-II data collected, providing 17 unique energies from 3-200 GeV with some overlapping collider and FXT energies
- Precision analyses are ongoing with very well understood detector
- Exciting physics program

Future:

- Forward upgrade (silicon detectors + calorimetry)
- 2022-25: p+p, p+Au, Au+Au at 200 GeV and p+p at 510 GeV